The Hubbard model with bond-charge interaction on a triangular lattice: a renormalization group study

1999 J. Phys.: Condens. Matter 11 3513

(http://iopscience.iop.org/0953-8984/11/17/309)

J. Phys.: Condens. Matter **11** (1999) 3513–3523. Printed in the UK PII: S0953-8984(99)99224-X

The Hubbard model with bond–charge interaction on a triangular lattice: a renormalization group study

Bibhas Bhattacharyya† and Shreekantha Sil‡

† Department of Physics, Scottish Church College, 1 & 3 Urquhart Square, Calcutta 700 006, India

† Institut für Theoretische Physik, Universität zu Köln, Zülpicher Strasse 77, D-50937, Köln, Germany

Received 11 November 1998, in final form 12 February 1999

Abstract. We have studied the Hubbard model with bond–charge interaction on a triangular lattice for a half-filled band. At the point of particle–hole symmetry the model could be analysed in detail in two opposite regimes of the parameter space. Using a real-space renormalization group (RG) we calculate the ground-state energy and the local moment over the whole parameter space. The RG results obey the exact results in the respective limits. In the intermediate region of the parameter space, the RG results clearly show the effects of the non-bipartite geometry of the lattice as well as the absence of symmetry in the reversal of the sign of the hopping matrix element.

1. Introduction

In spite of extensive efforts over the last few years, the problem of electronic correlation in low-dimensional systems remains to be clearly understood. Models of interacting electrons are difficult to handle in one and two dimensions owing to strong fluctuations. While there are a few exact solutions for one dimension (1-D) [1] and infinite dimensions [2], the situation is worse for two dimensions (2-D). Standard techniques like mean-field approximation or perturbative calculations are of very limited use in treating the intermediate-to-strong correlation in low-dimensional systems which are typically dominated by strong fluctuations. Numerical simulations and exact diagonalizations are also limited to small cluster sizes, because the dimension of the Hilbert space soon becomes too large to be handled as one goes from one to two dimensions. Therefore, it seems a worthwhile enterprise to apply an approximate real-space renormalization group (RG) known as the block RG (BRG) [3, 4] in this context. This works reasonably well for 1-D systems [5–7] and over the whole range of the coupling constants. This method employs a truncation of the Hilbert space, retaining a few low-lying states only, to bring out the essential ground-state properties. Although the efficacy of the truncation procedure is much more satisfactorily handled in a recently developed RG scheme known as the density-matrix RG (DMRG) method [8], the latter is yet to be developed for a truly 2-D system. The BRG method has already been applied to interacting electrons in 2-D [9] but only for bipartite lattices. It is interesting to see how it works in the case of a non-bipartite lattice like the triangular one. On the other hand, the problem of interacting electrons on a triangular lattice has been addressed for a long time [10–13] in view of the rich phase structure including the possibility of frustration [14]. In particular, ^{3}He on graphite was considered to be a good example of the Hubbard model [15] on a triangular lattice [10]. Recent work on

0953-8984/99/173513+11$19.50

organic superconductors like κ-BEDT-TTF compounds also investigates the phase diagrams of interacting-electron models on anisotropic triangular lattices [16].

In the present work we study a generalized Hubbard model with bond–charge interaction on the 2-D triangular lattice at half-filling by using the BRG. In section 2 we present the model and the renormalization scheme as suitably adapted to the present problem. Section 3 summarizes some of the exact solutions of this problem in limiting cases. In section 4 we focus on our results obtained from the RG study and make comparisons with the exact solutions. Section 5 concludes the present work.

2. The model and the RG scheme

The generalized Hubbard model with bond–charge interaction is defined as follows:

$$H = -t \sum_{\langle ij\rangle,\sigma} c^{\dagger}_{i\sigma} c_{j\sigma} + X \sum_{\langle ij\rangle,\sigma} c^{\dagger}_{i\sigma} c_{j\sigma} (n_{i-\sigma} + n_{j-\sigma}) - \mu \sum_i n_i + U \sum_i n_{i\uparrow} n_{i\downarrow} \tag{1}$$

where $c^{\dagger}_{i\sigma}$ ($c_{i\sigma}$) creates (annihilates) a particle with spin σ in a Wannier orbital located at the site i; the corresponding number operator is $n_{i\sigma} = c^{\dagger}_{i\sigma} c_{i\sigma}$. Here $n_i = n_{i\sigma} + n_{i-\sigma}$. The sum over $\langle ij\rangle$ denotes contributions from distinct nearest-neighbour pairs of sites on a triangular lattice. μ is the chemical potential. We focus our attention on the special case with $X = t$ for which the present model becomes particle–hole (p–h) symmetric even on the triangular lattice. In fact it has been shown that for some realistic systems $X \simeq t$ [17]. Furthermore, the choice $X = t$ results in some simplification in implementing the RG scheme and forces $\mu = U/2$ for half-filling. Moreover, at this special value of X we have some exact results for comparison. One should remember, however, that there is no $t \to -t$ symmetry due to the non-bipartite nature of the lattice.

Now, for $X = t$ and for a half-filled band ($\langle n_i\rangle = 1$) one can put $\mu = U/2$ and rewrite the Hamiltonian (2) as follows:

$$H = -t \sum_{\langle ij\rangle,\sigma} c^{\dagger}_{i\sigma} c_{j\sigma} (1 - n_{i-\sigma} - n_{j-\sigma}) + U \sum_i \left(\frac{1}{2} - n_{i\uparrow}\right)\left(\frac{1}{2} - n_{i\downarrow}\right) + D \sum_i \mathbf{1}_i + \frac{U}{2} N \tag{2}$$

where the constant $D = -\mu/2$ will account for the renormalization of the vacuum energy. Here we have added a constant term $NU/2$ to the Hamiltonian given by (1) to compensate for the chemical potential term subtracted therefrom. We just keep aside this constant term for the purpose of renormalizing the parameters in the Hamiltonian and then add the same constant to the ground-state energy at the end. The Hamiltonian has several conserved quantities: total number of particles ν, total spin S and the z-component S_z of the total spin, besides the p–h symmetry pointed out earlier. We divide the 2-D lattice with N sites into $N/3$ triangular blocks of three sites each (figure 1). The block Hamiltonian is then diagonalized for the three-site block. Since we are interested in the ground-state properties of the system we truncate the Hilbert space for the three-site blocks and retain only four low-lying states of the block Hamiltonian governed by the symmetries mentioned above together with the point group symmetry of the block. It is easy to see that the block Hamiltonian is block diagonalizable in terms of the good quantum numbers ν, S and S_z. The states with $\{\nu = 2, S = S_z = 0\}$, $\{\nu = 3, S = S_z = 1/2\}$, $\{\nu = 3, S = -S_z = 1/2\}$ and $\{\nu = 4, S = S_z = 0\}$ are considered for this purpose. Of these, the states in the first and the fourth group are connected by the p–h symmetry while those in the second and third are connected by spin-reversal symmetry. However, the point group symmetry in the 2-D lattice imposes further restriction on the choice of the states [9].

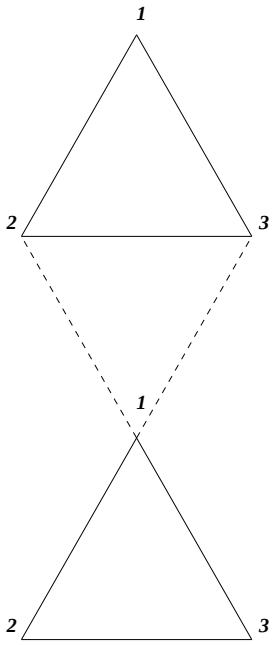

Figure 1. Two neighbouring triangular blocks used in the BRG method. The sites are numbered in an anticlockwise direction. Broken lines show the two connecting paths between the two blocks. One has to calculate contributions (identical for symmetry-adapted blocks) from both of the bonds in calculating the renormalized hopping (3).

To resolve this point we consider the symmetry group C_{3v} [18] of the basic triangular block. We take our eigenstates of the block Hamiltonian to also be the eigenstates of $R(C_{3v})$, the matrix representations of the group elements of C_{3v}. When choosing the four states to be retained, we simply take one from each of the four groups, so that all of them lie in the same representation of C_{3v}, such that the contribution to the ground-state energy be the minimum. This leads to the following RG equations which relate the renormalized parameters (primed quantities) to the original parameters (unprimed ones) in the Hamiltonian:

$$\begin{aligned} U' &= 2(E_2 - E_3) \\ D' &= 3D + (E_2 + E_3)/2 \\ t' &= 2\,\mathrm{Re}[\lambda^*(\lambda - 2\lambda')]t \end{aligned} \tag{3}$$

where E_2 and E_3 are the lowest eigenvalues in the subspaces $\{\nu = 2, S = S_z = 0\}$ and $\{\nu = 3, S = S_z = 1/2\}$, respectively; and

$$\begin{aligned} \lambda &= \langle \nu = 2, S = S_z = 0 | c_{b\uparrow} | \nu = 3, S = S_z = \tfrac{1}{2} \rangle \\ \lambda' &= \langle \nu = 2, S = S_z = 0 | c_{b\uparrow} n_{b\downarrow} | \nu = 3, S = S_z = \tfrac{1}{2} \rangle. \end{aligned} \tag{4}$$

λ^* is the complex conjugate of λ and Re denotes the real part. Here the subscript b refers to the site index of a *boundary* site of the block. For a triangular block, however, this could be any of the three sites. The factor of 2 appears in the renormalization of the hopping due to there being two connecting paths between the two neighbouring three-site blocks (figure 1). We illustrate the scheme of the RG calculations using the recursion relations (3) in the appendix.

Using these recursion relations, one can find out the ground-state energy E_0 from

$$E_0 = \lim_{n\to\infty} D^{(n)} + NU/2$$

where the superscript refers to the nth stage of iteration. The term $NU/2$ in the above expression comes from the constant term added in (2). One could study the recursion of any suitable operator to calculate any other physical quantity within this approximation. For example, we calculate the local moment L_0 given by

$$L_0 = \frac{3}{4}(n_\uparrow - n_\downarrow)^2.$$

The recursion relation for L_0 turns out to be

$$L_0 = A + BL_0'$$

where A and B are numbers depending on the components of the basis states retained in course of basis truncation. Since all three sites in the basic triangular block are in the same status (after adapting the C_{3v} symmetry), one can use any of them for finding the recursion of L_0.

Table 1. The energies of the eigenstates of the block Hamiltonian corresponding to $\nu = 2$ and $\nu = 3$ are E_2 and E_3, respectively. These are tabulated for different possible combinations of states belonging to different irreducible representations of C_{3v}. We adopt standard group theoretical notation [18] (A_i for 1-D irreducible representations and E for the 2-D one).

Combination given by irreducible representation	E_2	E_3	$E_2 + E_3$
A_1	$-2t - U/4$	$U/4$	$-2t$
A_1	$3U/4$	$U/4$	U
E	$t - U/4$	$-3U/4$	$t - U$
E	$t - U/4$	$-\sqrt{3}t + U/4$	$(\sqrt{3}+1)t$
E	$t - U/4$	$\sqrt{3}t + U/4$	$-(\sqrt{3}-1)t$
E	$3U/4$	$-3U/4$	0
E	$3U/4$	$-\sqrt{3}t + U/4$	$\sqrt{3}t + U$
E	$3U/4$	$\sqrt{3}t + U/4$	$\sqrt{3}t + U$

It is interesting to note that due to the group theoretical restriction on the choice of the truncated basis it is not possible, in general, to select the lowest-energy states from all of the four groups at a time. The states with the lowest energies in all four groups do not necessarily belong to the same irreducible representation of C_{3v}. If such states are retained, then the matrix element λ defined in (4) will be zero. So instead of the states with lowest energy one targets the states belonging to the same irreducible representation. This problem did not arise in the 1-D cases. Therefore, it is possible here to choose any of the possible combinations of four states (from the four groups) compatible with the symmetry group. Again, from (3), one can see that the contribution to the ground-state energy from each iteration is $\propto E_2 + E_3$. Then it is natural to seek for the combination which gives the lowest value of this quantity. However, one should be careful about the value of the renormalized hopping t' thus generated, because this in turn will seriously affect the contribution to the energy in the subsequent iteration. We have, therefore, taken into consideration all of the possible channels permitted by the symmetry group up to three subsequent iterations and then considered the energetically most favourable ones for the next iterations. For example, consider the case in which we have an optimum choice of five distinct channels (each with a unique set of four states belonging to a given irreducible representation) to start with. In three successive iterations it gives rise to 125 ($=5 \times 5 \times 5$) channels out of which we retain the best 25 for the next step. This is an optimized way to achieve the true ground state. Different possible combinations of the two- and three-particle states are shown in table 1 in terms of the irreducible representation, as are the corresponding energies E_2 and E_3. It is evident from the table that the contribution $(E_2 + E_3)/2$ to the constant

term D in the Hamiltonian (2) makes just a few combinations advantageous in constructing the RG scheme.

3. Exact results for the model

The exact ground-state energy could be calculated for the present model (2) in two opposite extremal ranges of the parameter space in U/t. To do this, we try to match a variational upper bound $E_{\rm up}$ to the exact energy to a lower bound $E_{\rm lo}$. To find the upper bound $E_{\rm up}$ we choose a trial state $|\Psi_{\rm trial}\rangle$ and calculate, by the variational principle,

$$E_{\rm up} = \frac{\langle\Psi_{\rm trial}|H|\Psi_{\rm trial}\rangle}{\langle\Psi_{\rm trial}|\Psi_{\rm trial}\rangle}.$$

To calculate the lower bound $E_{\rm lo}$, we break up the Hamiltonian (2) into a sum of the cluster Hamiltonians corresponding to the smallest triangular clusters. These could be exactly diagonalized. Then, again by the variational principle, $E_{\rm lo}$ is given by

$$E_{\rm lo} = \sum_{\alpha} E^{\alpha}_{\rm min} + C$$

where $E^{\alpha}_{\rm min}$ is the lowest eigenvalue for the αth cluster and C is the constant term, if there is one, appearing in the Hamiltonian. To find the lower bound, we rewrite the Hamiltonian (1) in the following form:

$$H = \sum_{\alpha=1}^{2N}\left[-\frac{t}{2}\sum_{\langle ij\rangle\in\alpha,\sigma} c^{\dagger}_{i\sigma}c_{j\sigma}(1-n_{i-\sigma}-n_{j-\sigma}) + \frac{U}{12}\sum_{i\in\alpha}(n_{i\uparrow}-n_{i\downarrow})^2\right] + \frac{U}{2}N$$
$$= \sum_{\alpha=1}^{2N} H_{\rm cluster}(\alpha) + \frac{U}{2}N \tag{5}$$

where we have used $\mu = U/2$ and compensated for this by adding a term $NU/2$, N being the number of lattice sites. So, here, $C = NU/2$. In the above form of the Hamiltonian we have summed over all possible ($2N$ in number) triangular clusters α. The fractional numbers appearing with t and U are due to the over-counting of the bonds (twice each) and the sites (each being shared by six adjacent triangles). $H_{\rm cluster}(\alpha)$ is the cluster Hamiltonian of the αth cluster for which we have to find the lowest eigenvalue $E^{\alpha}_{\rm min}$.

Table 2. Eigenvalues of the cluster Hamiltonian $H_{\rm cluster}(\alpha)$ as given in (5) corresponding to different number (ν) of particles.

ν	Energy
0, 6	0
1, 5	$-t-U/12$, $t/2-U/12$
2, 4	0, $-t-U/6$, $t/2-U/6$
3	$\pm t-U/12$, $-U/4$, $\pm t/2-U/12$

We categorize the results into two regimes as follows:

(a) $U > 0$: for very large positive values of U the system is expected to go over to a phase with singly occupied sites [17]. We choose the trial wavefunction as

$$|\Psi\rangle = \prod_{i\in\mathcal{L}} c^{\dagger}_{i\uparrow}\prod_{j\in\mathcal{L}'} c^{\dagger}_{j\downarrow}|0\rangle \tag{6}$$

where $|0\rangle$ is a site vacuum and $\mathcal{L}$ and $\mathcal{L}'$ are arbitrary disjoint sets of lattice sites, each containing $N/2$ lattice points, which together build up the whole lattice. Using this $|\Psi\rangle$,

we obtain an upper bound $E_{\rm up} = 0$. We find the different energy eigenvalues belonging to different values of ν in a basic triangular plaquette α to be as shown in table 2. Now the lowest of these, $E^{\alpha}_{\rm min}$, will be $-U/4$ if

$$-U/4 \leqslant \mathrm{Min}\,[\pm t - U/12, \pm t/2 - U/12, -t - U/6, t/2 - U/6, 0]\,. \tag{7}$$

This is true for $U \geqslant 12|t|$. Then $E_{\rm min} = -U/4$. Consequently, $E_{\rm lo} = 2N \times (-U/4) + NU/2 = 0 = E_{\rm up}$.

So, in the $U > 0$ sector, the exact ground-state energy $E_0 = 0$ for $U \geqslant 12|t|$ and the ground state becomes a paramagnetic insulator with all sites singly occupied.

(b) $U < 0$: here we choose the trial wavefunction as follows:

$$|\Psi\rangle = \prod_{i\in\mathcal{L}} c^{\dagger}_{i\uparrow} c^{\dagger}_{i\downarrow} |0\rangle \tag{8}$$

where $\mathcal{L}$ denotes a set of arbitrarily chosen $N/2$ sites. This choice gives $E_{\rm up} = NU/2$. Now using the possible values of the lowest energies in a triangular plaquette as listed in table 2, we find that $E_{\rm min} = 0$ if

$$0 \leqslant \mathrm{Min}\,[\pm t - U/12, \pm t/2 - U/12, -t - U/6, t/2 - U/6, -U/4]\,. \tag{9}$$

This corresponds to $U \leqslant -12|t|$ and consequently $E_{\rm lo} = NU/2 = E_{\rm up}$.

So, in the $U < 0$ sector, the exact ground-state energy $E_0 = NU/2$ for $U \leqslant -12|t|$ and the ground state becomes an insulator composed of $N/2$ 'doublons'.

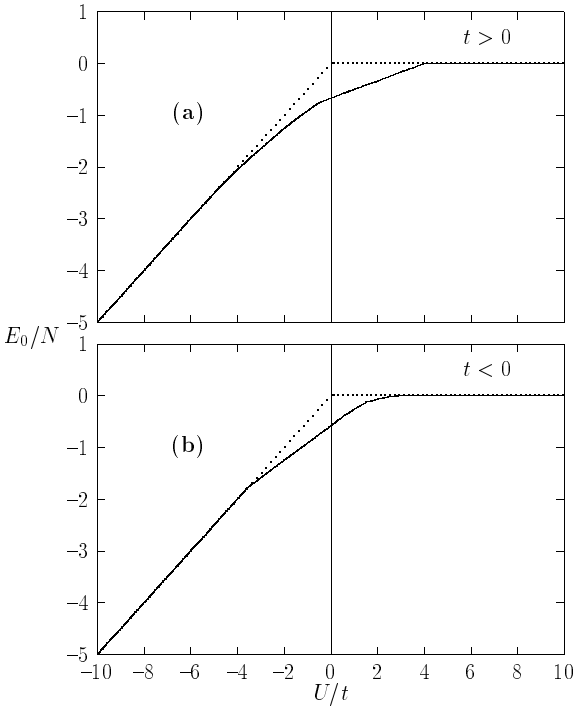

Figure 2. A plot of E_0/N, the ground-state energy per site, as a function of U/t for (a) $t > 0$ and (b) $t < 0$. The dotted lines correspond to $E_0 = NU/2$ for $U/t \leqslant 0$ and $E_0 = 0$ for $U/t \geqslant 0$ and thus show the asymptotic exact results in the respective limits.

4. Results obtained in the RG scheme

The ground-state energy as a function of the coupling constant U/t, calculated in the RG scheme, is shown in figures 2(a) and 2(b) for the two cases $t > 0$ and $t < 0$, respectively. It appears that the curves agree completely with the asymptotic solutions given above. In fact, E_0 reaches the zero value well before the threshold value of U, $U_{c_1} = 12|t|$, as one increases the value of U/t. However, there appears a difference between the two values of U_{c_1} for $t > 0$ and $t < 0$. This merely reflects the lack of $t \to -t$ symmetry owing to the tripartite nature of the lattice. Also, on the other side of $U/t = 0$ the energy curves are in complete agreement with the available exact results. Here also, E_0 takes the value $NU/2$ at a much higher value of U compared to the threshold value $U_{c_2} = -12|t|$ as the value of U/t is decreased. It appears that the wide region in the parameter space ($-12|t| \leqslant U \leqslant 12|t|$) for which the exact solution could not be obtained is much narrower in reality. The energy curve obtained in the RG calculation smoothly interpolates between the two exactly solvable opposite limits. In the intermediate region we find that $t > 0$ always gives the lower energy. This can be checked against a naive calculation for any reasonable size of a cluster having a triangular geometry.

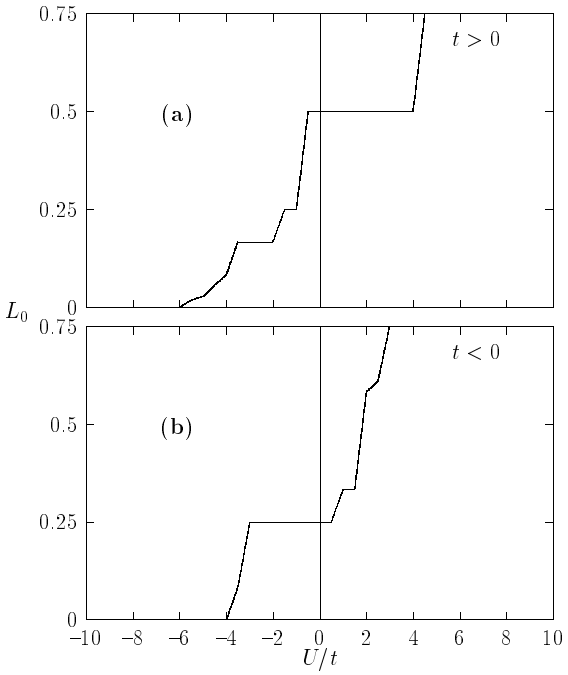

Figure 3. A plot of the local moment L_0 as a function of U/t for (a) $t > 0$ and (b) $t < 0$.

The local moment, which measures the proliferation of 'doublons' in the ground state, is plotted against U/t for $t > 0$ and $t < 0$ in figures 3(a) and 3(b), respectively. As we can readily see, the singly occupied insulating phase given by the wavefunction (6) corresponds to $L_0 = 3/4 = 0.75$ for $U \geqslant 12|t|$. Similarly, for $U \leqslant -12|t|$, the wavefunction (8) corresponds to $L_0 = 0$. These are reproduced in the RG scheme in accordance with the energy curves. The parameter space in between these two insulating phases shows a non-trivial discrepancy between the cases $t > 0$ and $t < 0$. A large plateau at $L_0 = 0.5$ appears for $t > 0$ which is totally absent in the case of $t < 0$. For the latter we find a wide plateau at $L_0 = 0.25$. Other

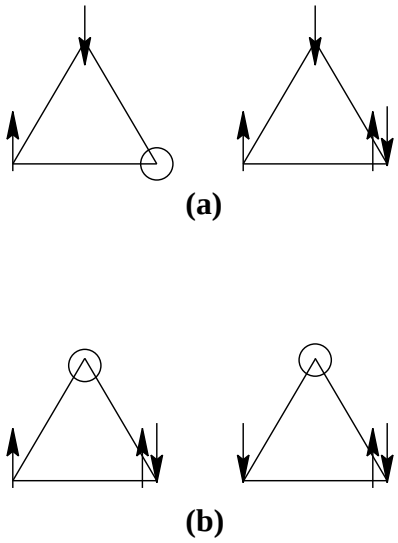

Figure 4. The energetically most favourable configurations in a three-site cluster for a typical point in the metallic region, $U = |t| = 1$. (a) Configurations with $\nu = 2, 4$ dominate for $t > 0$. Such configurations correspond to $L_0 = 0.50$. (b) Configurations with $\nu = 3$ dominate for $t < 0$, corresponding to $L_0 = 0.25$. In this schematic figure, $\uparrow$ ($\downarrow$) stands for an electron with 'up spin' ('down spin') at a given Wannier orbital. $\circ$ denotes an empty site.

small structures in the local moment curves may be consequences of finite-size effects. The plot of the local moment clearly shows that the extents of pairing (in the form of doublons) are different in the two cases, although both of them possibly correspond to a metallic ground state. It is important to note that such a metallic phase in the same model on a 1-D chain gives a free-fermionic local moment $L_0 = 0.375$ [6]. These plots also show that the phase transitions occurring at U_{c_1} and U_{c_2} are abrupt as in the 1-D case [6]. The departure from $L_0 = 0.375$ in the metallic case is a consequence of the lattice geometry. To naively illustrate this point, let us consider the specific case of $U = |t| = 1.0$. As one can readily check from table 2, the lowest energy in each triangular plaquette α comes from $\nu = 2, 4$ if $t > 0$; typical configurations corresponding to this are shown in figure 4(a). Clearly, such configurations will dominate in the global wavefunction and the value of L_0 will be pushed towards 0.5. On the other hand, a similar observation reveals that in case of $t < 0$, the lowest contribution comes from the $\nu = 3$ sector with configurations similar to those shown in figure 4(b). These obviously lower the value of L_0 towards 0.25. In reality, however, L_0 is slightly greater than 0.25 at this point for $t < 0$, as one can see from figure 3(b). This is because of the mixing of other configurations for optimization of the hopping process between different clusters. Also, there might be finite-size effects.

The difference between the values of U_{c_2} for $t > 0$ and $t < 0$ is distinctly visible from the plots of the local moment. Thus the local moment plot very clearly captures the lack of $t \to -t$ symmetry which is essential for the lattice under consideration.

5. Conclusions

Summarizing, we have studied the Hubbard model with the bond–charge interaction on a triangular lattice at the special point of particle–hole symmetry. At this point we obtain exact

results in two opposite limits of the parameter space. The system behaves as a paramagnetic insulator above a certain value U_{c_1} of the on-site correlation. Below the critical value U_{c_2} it undergoes a transition to an insulating state of disordered doublons. To explore the full parameter space we employ a real-space version of the RG. The RG scheme is suitably adapted for this purpose. The ground-state energy and the local moment values calculated in the RG scheme reproduce the exact results as they did in the 1-D case [6] too. This lends some support to the present RG approximations. In the intermediate range of the parameter space, where no exact solution has been available, the RG results indicate that the degree of pairing (in terms of the formation of local doublons) is different from that in the 1-D counterpart of this problem. The triangular geometry plays a crucial role there. Moreover, in this region, both the energy and the local moment plots show up the effect of losing the $t \rightarrow -t$ symmetry. The parameter space between U_{c_1} and U_{c_2}, corresponding to a possible metallic phase (as it did in the 1-D counterpart [6, 19]), appears to be less wide in the RG calculations compared to the exact solution. The present study gives an indication that the RG scheme used here could be successfully applied to other cases in 2-D. Extension to the cases with $X \neq t$ seems interesting, although it is well known that the lack of particle–hole symmetry creates some problem with the present form of the RG on a non-bipartite lattice. It is interesting to look for the short-ranged correlations, if any, in the intermediate region of the parameter space. It is also interesting to know the effect of the finite block size on the satellite plateaus in the local moment plot; this requires a larger block in the RG analysis (a body-centred hexagon is the next choice after a triangle). However, the convergence of the RG results to the exact ones is often slow with increasing block size, and the effect of the discarded states may be important in determining the global wavefunction [8, 20]. Therefore, a better way of supplementing the present study is to use the DMRG algorithm, which can take into account a larger number of configurations within a block in a controlled and systematic way. Of course, the DMRG algorithm has to be suitably adapted (to a 2-D lattice in the thermodynamic limit) for this purpose.

Acknowledgments

One of the authors (SS) acknowledges the financial support given by Sonderforschungsbereich 341 supported by the Deutsche Forschungsgemeinschaft (DFG). Computational facilities enjoyed at the Saha Institute of Nuclear Physics, Calcutta, are also gratefully acknowledged.

Appendix

In the present appendix we give a brief sketch of the derivation of the recursion relation (3) quoted in the text. We have retained a suitable state of low energy in each of the subspaces $\{\nu = 2, S = S_z = 0\}$, $\{\nu = 3, S = S_z = \frac{1}{2}\}$, $\{\nu = 3, S = -S_z = \frac{1}{2}\}$ and $\{\nu = 4, S = S_z = 0\}$. These states are designated $|0'\rangle$, $|\uparrow'\rangle$, $|\downarrow'\rangle$ and $|\uparrow\downarrow'\rangle$, respectively. Let the corresponding energy eigenvalues be $E_{0'}$, $E_{\uparrow'}$, $E_{\downarrow'}$, $E_{\uparrow\downarrow'}$, respectively. As we have mentioned earlier, the first and the fourth states are connected by the particle–hole symmetry while the second and the third are connected by spin-reversal symmetry. It follows, therefore, that $E_{0'} = E_{\uparrow\downarrow'} = E_2$ and $E_{\uparrow'} = E_{\downarrow'} = E_3$. These four states closely resemble the single-site states $|0\rangle$, $|\uparrow\rangle$, $|\downarrow\rangle$ and $|\uparrow\downarrow\rangle$ in that the spin quantum numbers are the same and there is a one-to-one correspondence between the total number of electrons, ν, in such a state and the occupation number of the corresponding single-site state (they differ by two). We, therefore, identify a three-site block as a 'renormalized' site in the scaled lattice and the retained states of the three-site block as

the 'renormalized' single-site states [3, 4].

The intrablock Hamiltonian could be written within the subspace of the truncated basis in terms of the new block-fermion operators:

$$H_0' = \frac{1}{2}(E_2 + E_3) + 2(E_2 - E_3)\left(\frac{1}{2} - n_{\uparrow'}\right)\left(\frac{1}{2} - n_{\downarrow'}\right) \tag{A.1}$$

where the prime denotes the renormalized block-fermion operators. Comparison of this 'renormalized' block Hamiltonian with the single-site part of the Hamiltonian (2) leads to the renormalization formulae for U and D in (3).

To obtain the interblock part of the Hamiltonian, we calculate the matrix elements of the old fermion operators at the boundary site b, $c_{b\uparrow}$ and $c_{b\uparrow}n_{b\downarrow}$, connecting the states that we have retained. This leads to the renormalization of t as follows:

$$t' = 2(\lambda\lambda^* - \lambda\lambda'^* - \lambda'\lambda^*) \tag{A.2}$$

which is equivalent to the last relation in (3). λ and λ' were already given in (4).

Let us now illustrate the scheme of calculation of the renormalized parameters as given by equation (3). We refer to a specific case with a choice of states belonging to the E representation (table 1) from all of the subspaces. We find from table 1 that there could be several sets of states from the subspaces with $\nu = 2$ and $\nu = 3$, i.e. with eigenvalues E_2 and E_3 respectively. For example, we pick up the case with $E_2 = t - U/4$ and $E_3 = -3U/4$.

The block state $|0'\rangle$ (with $S_z = 0$ and $\nu = 2$), which is an eigenvector of the block Hamiltonian belonging to the eigenvalue $E_2 = t - U/4$ and is simultaneously an eigenvector of the rotation operators $R(C_{3v})$, is given by

$$|0'\rangle = \frac{1}{2\sqrt{6}}[|0\uparrow\downarrow\rangle - |0\downarrow\uparrow\rangle - 2|\uparrow 0\downarrow\rangle + 2|\downarrow 0\uparrow\rangle + |\uparrow\downarrow 0\rangle - |\downarrow\uparrow 0\rangle] + \frac{\mathrm{i}}{2\sqrt{2}}[|0\uparrow\downarrow\rangle - |0\downarrow\uparrow\rangle - |\uparrow\downarrow 0\rangle + |0\downarrow\uparrow\rangle]. \tag{A.3}$$

Similarly, the block state $|\uparrow'\rangle$ (with $S_z = 1/2$ and $\nu = 3$), which is an eigenvector of the block Hamiltonian belonging to the eigenvalue $E_3 = -3U/4$ and is simultaneously an eigenvector of the rotation operators $R(C_{3v})$, is given by

$$|\uparrow'\rangle = \frac{1}{2\sqrt{3}}[|\uparrow\downarrow\uparrow\rangle - 2|\uparrow\uparrow\downarrow\rangle + |\downarrow\uparrow\uparrow\rangle] + \frac{\mathrm{i}}{2}[|\uparrow\downarrow\uparrow\rangle - |\downarrow\uparrow\uparrow\rangle]. \tag{A.4}$$

Here we have expressed a given configuration of the triangular block by $|\beta\gamma\delta\rangle$ (where $\beta, \gamma, \delta = 0, \uparrow, \downarrow$ or $\uparrow\downarrow$) such that the configuration obeys the ordering of the site indices $1 \to \beta$, $2 \to \gamma$ and $3 \to \delta$ (see figure 1 for the site indices).

For the choice of these particular sets of states,

$$\lambda = \langle 0'|c_{1\uparrow}|\uparrow'\rangle = -\frac{1}{2\sqrt{2}} + \frac{\mathrm{i}}{2\sqrt{6}}$$

while

$$\lambda' = \langle 0'|c_{1\uparrow}n_{1\downarrow}|\uparrow'\rangle = 0.$$

λ' may have a non-zero value for other sets of states. Instead of using $c_{1\uparrow}$ and $n_{1\uparrow}$, one could use operators belonging to site No 2 or No 3 to finish up with the same result. This is because all three sites are 'boundary sites' (as pointed out earlier) and, therefore, equivalent to each other. These lead to the following RG equations:

$$\begin{aligned} U' &= 2(E_2 - E_3) = 2t + U \\ D' &= 3D + (E_2 + E_3)/2 = 3D + t/2 - U/2 \\ t' &= 2\,\mathrm{Re}[\lambda^*(\lambda - 2\lambda')]t = \tfrac{1}{6}t. \end{aligned} \tag{A.5}$$

The renormalized parameters could be easily calculated in a similar way for any other choice of states shown in table 1.

References

[1] Lieb E and Wu F 1968 *Phys. Rev. Lett.* **20** 1445
[2] Vollhardt D 1993 *Correlated Electron Systems* vol 9, ed V J Emery (Singapore: World Scientific)
[3] Hirsch J E 1980 *Phys. Rev.* B **22** 5259
[4] Dasgupta C and Pfeuty P 1981 *J. Phys. C: Solid State Phys.* **14** 717
[5] Bhattacharyya B and Roy G K 1995 *J. Phys.: Condens. Matter* **7** 5537
[6] Bhattacharyya B and Sil S 1995 *J. Phys.: Condens. Matter* **7** 6663
Bhattacharyya B and Sil S 1996 *J. Phys.: Condens. Matter* **8** 911
[7] Sil S and Bhattacharyya B 1997 *Phys. Rev.* B **54** 14 349
[8] White S R 1992 *Phys. Rev. Lett.* **69** 2863
White S R 1993 *Phys. Rev.* B **48** 10 345
[9] Perez-Conde J and Pfeuty P 1993 *Phys. Rev.* B **47** 856
Vanderzande C 1985 *J. Phys. A: Math. Gen.* **18** 889
[10] Machida K and Fujita M 1990 *Phys. Rev.* B **42** 2673
[11] Krishnamurthy H R, Jayaprakash C, Sarker S and Wenzel W 1990 *Phys. Rev. Lett.* **64** 950
Jayaprakash C, Krishnamurthy H R, Sarker S and Wenzel W 1991 *Europhys. Lett.* **15** 625
[12] Kato M and Kokubo F 1994 *Phys. Rev.* B **49** 8864
[13] Pecher U and Büttner H 1995 *Z. Phys.* B **98** 239
[14] Gazza C J, Trumper A E and Ceccatto H A 1994 *J. Phys.: Condens. Matter* **6** L624
[15] Hubbard J 1963 *Proc. R. Soc.* A **276** 238
[16] Kino H and Kotani H 1998 *J. Phys. Soc. Japan* **67** 3691
(Kino H and Kotani H 1998 *Preprint* cond-mat/9807147)
Kondo H and Moriya T 1998 *Preprint* cond-mat/9807322
[17] Strack R and Vollhardt D 1993 *Phys. Rev. Lett.* **17** 2637
[18] Cotton F A 1971 *Chemical Applications of Group Theory* 2nd edn (New York: Wiley)
[19] Arrachea L and Aligia A A 1994 *Phys. Rev. Lett.* **73** 2240
[20] Bhattacharyya B and Sil S 1996 *Phys. Lett.* A **210** 129